DNA hypermethylation enhanced telomerase reverse transcriptase expression in human induced pluripotent stem cells

Ken Takasawa[1], Yoshikazu Arai[1], Mayu Yamazaki-Inoue[2], Masashi Toyoda[3], Hidenori Akutsu[2], Akihiro Umezawa[2], Koichiro Nishino[1, 4*]

[1] Laboratory of Veterinary Biochemistry and Molecular Biology, Graduate School of Medicine and Veterinary Medicine/Faculty of Agriculture, University of Miyazaki, 1-1 Gakuen-Kibanadai-Nishi, Miyazaki, 889-2192, Japan.

[2] Center for Regenerative Medicine, National Research Institute for Child Health and Development, 2-10-1 Okura, Setagaya-ku, Tokyo 157-8535, Japan.

[3] Research Team for Geriatric Medicine (Vascular Medicine), Tokyo Metropolitan Institute of Gerontology, 35-2 Sakaemachi, Itabashi-ku, Tokyo 173-0015, Japan.

[4] Center for Animal Disease Control, University of Miyazaki, 1-1 Gakuen-Kibanadai-Nishi, Miyazaki, 889-2192, Japan.

* Corresponding author

Koichiro Nishino

E-mail: aknishino@cc.miyazaki-u.ac.jp

Tel: +81-985-58-7263

Fax: +81-985-58-7263

Abstract

During reprogramming into human induced pluripotent stem cell (iPSCs), several stem cell marker genes are induced, such as *OCT*-4, *NANOG*, *SALL4*, and *TERT*. *OCT-4, NANOG*, and *SALL4* gene expression can be regulated by DNA methylation. Their promoters become hypomethylated in iPSCs during reprogramming, leading to their induced expression. However, epigenetic regulation of the *TERT* gene remains unclear. In this study, we focused on epigenetic regulation of the human *TERT* gene and identified a differentially methylated region (DMR) at a distal region in the *TERT* promoter between human iPSCs and their parental somatic cells. Interestingly, the *TERT*-DMR was highly methylated in iPSCs, but low-level methylation was observed in their parental somatic cells. Region-specific, methylated-promoter assays showed that the methylated *TERT*-DMR up-regulated the promoter activity in iPSCs. In addition, Lamin B1 accumulated at the *TERT*-DMR in iPSCs, but not in their parent somatic cells. These results suggested that the *TERT* transcription was enhanced by DNA methylation at the *TERT*-DMR via binding to nuclear lamina during reprogramming. Our findings shed light on a new functional aspect of DNA methylation in gene expression.

Keywords

Human *TERT* gene; Human iPSCs; DNA methylation; Epigenetics; Lamin B1; Reprogramming

Introduction

Telomerase reverse transcriptase (TERT) is a key component of telomerase and an important molecule for stem cells. TERT elongates telomere sequences at the ends of chromosomes and defines the high proliferative capacity of stem cells. The human *TERT* gene is highly expressed in induced pluripotent stem cells (iPSCs), but not somatic cells. Therefore, activation of the *TERT* gene is essential for reprogramming human somatic cells into iPSCs [1].

Reprogramming is accompanied with genome-wide epigenetic modifications. Genomic DNA methylation, one mode of epigenetic regulation, serves as an important mechanism in development and cell differentiation [2–5] as well as reprogramming in iPSCs. Stem cell marker genes, such as octamer-binding transcription factor 4 (*OCT-4*) [1], homeobox transcription factor NANOG (*NANOG*) [1] and SAL-like 4 (*SALL4*) [6], show tissue-specific demethylation corresponding to their expression during reprogramming. For instance, the CpG sites in the *OCT-4* promoter are kept hypomethylated, which permits its expression in pluripotent stem cells. In contrast, hypermethylation of the *OCT-4* promoter silences its expression in somatic cells. Therefore, the DNA methylation profiles of the *OCT-4* promoter has been used as an epigenetic marker of iPSC reprogramming [1,7]. Although *TERT* is a pluripotency marker gene in humans, the epigenetic regulation of human *TERT* gene by DNA methylation remains unclear.

In this study, we identified a differentially methylated region in the distal promoter of the human *TERT* gene. Hypermethylation of the *TERT* promoter induced its expression. We show here a novel epigenetic regulatory mechanism wherein hypermethylation of the *TERT* promoter was activated through binding to the nuclear membrane.

Materials and Methods

Human cell culture

Human endometrial (UtE1104) [8], amniotic (AM936EP) [9], menstrual blood cell (Edom22) [8], and fetal lung fibroblast (MRC-5) [10] cells were maintained in Poweredby10 medium (GlycoTechnica, Yokohama, Japan). Placental artery endothelial cells (PAE551) [9] were cultured in medium from the EGM-2MV BulletKit (Lonza, Walkersville, MD, USA) containing 5% fetal bovine serum. The human embryonal carcinoma NCR-G3 and NCR-G4 cell lines were cultured in G031101 medium, as previously described [11]. The human iPSC lines, MRC-iPS-25 [12], PAE-iPS-1 [13], AM-iPS-8 [9], UtE-iPS-6 [13], Edom-iPS-2 [13], and iPS-201B7 [1] were derived from the MRC-5, PAE551, AM963EP, UtE1104, Edom22 and HDF cell lines, respectively. iPSCs were maintained on irradiated mouse embryonic fibroblasts in KO-DMEM (Thermo Fisher Scientific, Inc., Waltham, MA, USA) containing 20% knockout-serum replacement (Thermo), supplemented with 1% GlutaMAX (Thermo), 1% nonessential amino acids (Thermo), 55 μM 2-mercaptoethanol (Thermo), 1% penicillin and streptomycin (Thermo) and 10 ng/ml recombinant human basic fibroblast growth factor (Wako Pure Chemical Industries, Ltd., Osaka, Japan). Frozen pellets of human embryonic stem cell lines (HUESCs) [14] were kindly gifted from Drs. C. Cowan and T. Tenzan (Harvard Stem Cell Institute, Harvard University, Cambridge, MA). For demethylation assays, MRC-iPSCs were cultured for 4 days in medium containing 0, 0.5, 1, or 5 μM 5-aza-2′-deoxycytidine (5-aza-dC, Merck Millipore, Billerica, MA, USA). The human cells used in study are summarized in Supplemental Table 1.

Gene expression analysis

For the reverse transcription-polymerase chain reaction (RT-PCR), first-strand cDNA was synthesized using total RNA (1 μg) with random hexamers and ReverTra Ace reverse

transcriptase (TOYOBO Co., Ltd., Osaka, Japan). The cDNA template was amplified using BIOTAQ™ HS DNA Polymerase (Bioline Ltd; London, UK) and specific primers for *TERT*, *POU5F1*, *NANOG*, *SOX2*, *SALL4*, *EPHA1*, and *GAPDH*. All PCR experiments were performed under the following thermocycling conditions: 95ºC for 10 min; 30 cycles of 95ºC for 30 s, 60ºC for 30 s, and 72ºC for 1 min; with a final extension at 72ºC for 10 min. Quantitative real-time PCR (qPCR) was performed using SYBR® Green PCR master mix (Applied Biosystems, Waltham, MA, USA). Data were normalized to GAPDH expression. Gene-expression levels are presented as the fold-change in expression, which was calculated using the $2^{-\Delta\Delta CT}$ method [15]. The sequences of primers used in this study are summarized in Supplemental Table 2.

Gene expression-array data were obtained from Gene Expression Omnibus microarray data archive (GEO; http://www.ncbi.nlm.nih.gov/geo/) (accession numbers GSE20750, GSE42099, and GSE24677) [13,16]. All expression data had been analyzed using the same platform, namely an Agilent-014850 Whole Human Genome Microarray 4x44K G4112F. The expression data were processed by median normalization, then used for our analysis.

Genome-wide DNA methylation analysis

Genome-wide DNA methylation analysis was performed using the Illumina Infinium HumanMethylation450K BeadChip Kit (Illumina Inc., San Diego, CA, USA) and the BeadChip was scanned on a BeadArray Reader (Illumina Inc.) according to the manufacturer's instructions. Methylated and unmethylated signals were used to compute a ß-value, which was a quantitative score of the DNA-methylation levels, ranging from "0.00" (completely unmethylated) to "1.00" (completely methylated). All DNA-methylation data were submitted to GEO under accession numbers GSE73938 and GSE99716.

Bisulfite sequencing

Sodium bisulfite treatment of genomic DNA was performed using the EZ DNA Methylation-Gold™ Kit (Zymo Research, Irvine, CA). PCR amplification was performed using BIOTAQ™ HS DNA Polymerase (Bioline Ltd) and specific primers for *TERT* promoters. All PCR experiments were performed under the following thermocycling conditions: 95ºC for 10 min; 40 cycles of 95ºC for 30 s, 55ºC for 30 s, and 72ºC for 1 min; with a final extension at 72ºC for 10 min. The sequences of primers used in this study are summarized in Supplemental Table 2. To determine the methylation states of individual CpG site at the *TERT* promoter, the PCR product was gel-extracted, subcloned into the pGEM-T Easy vector (Promega, Madison, WI), and sequenced. Methylation sites were visualized, and quality control was performed using the web-based tool, "QUMA" (http://quma.cdb.riken.jp/) [17].

Region-specific methylated *TERT* reporter assay

The 5′-flanking fragment of the human *TERT* gene was isolated from genomic DNA of MRC-iPSCs by genomic PCR. The position of the transcription start site (TSS) was designated as +1. The 1.6-kbp, 5′-flanking region (from –1,560 to +36) containing an EcoRI site at –625 nucleotides (nt) was cloned into pGL4.10-Basic vector (Promega). This construct was designated as *TERT*-1560. The *TERT*-626 construct was generated by removing the region from –1,560 to –625 from *TERT*-1560, following digestion with Acc65I (New England BioLabs [NEB], Beverly, MA) and EcoRI (NEB), and self-ligation. The *TERT*-1560_Me construct was generated by re-ligation of the fragment (from –1,560 to –625) that was methylated in vitro with SssI methylase (NEB). MRC-5 cells and MRC-iPSCs were co-transfected with the reporter constructs and pGL4.74[hRluc/TK], at a 6: 1 molar ratio in each case. Luciferase activities were determined using the Dual-Luciferase Reporter Assay system

(Promega) at 48 h post-transfection, according to the manufacturer's instructions. Promoter activity was normalized to Renilla luciferase activity. Assays were performed independently at least 3 times independently.

Chromatin immunoprecipitation (ChIP) assay

The cells were fixed with 1% formaldehyde for 10 min at room temperature and then incubated in 125 mM glycine for 10 min, to quench reactive aldehydes. The cells were collected after rinsing them with phosphate-buffered saline (PBS). The cells were lysed in lysis buffer (10 mM Tris-HCl [pH 8.0], 10 mM NaCl, and 0.2 % Triton-X) and sonicated until the chromatin fragments became 200 - 1,000 bp in size. The antibodies used for ChIP were as follows: anti-trimethylated histone H3 Lys 4 (H3K4me3, #MABI0004: MAB Institute Inc., Sapporo, Japan), anti-trimethylated histone H3 Lys 27 (H3K27me3, #17-622: Merck Millipore), anti-HP-1α (#2616: CST Inc., Danvers, MA, USA), and anti-Lamin B1 (#ab16048: Abcam, Cambridge, UK). Rabbit IgG (#PP64B: Merck Millipore) and mouse IgG (#12-371B: Merck Millipore) were used as negative controls to test the specificity of the ChIP results. After the ChIP step, the recovered chromatin samples were subjected to qPCR (ChIP-qPCR) using specific primers (Supplemental Table 2). The percent-input values were calculated as described previously [18]. The qPCR data for each primer pair were represented as percent-input by calculating each specific DNA fragment in immunoprecipitates relative to that in input DNA. The final values were determined by subtraction of the percent-input value obtained for a negative control immunoprecipitation with rabbit IgG or mouse IgG from the percent-input value of interest.

Statistical analysis

Differences between 2 independent samples were evaluated by performing two-tailed Student's t-test. All error bars represent the standard error of mean (SEM). Linear-regression analysis was used to analyze correlations between gene expression and DNA methylation.

Results and discussion

Identification of a differentially methylated region of the human *TERT* gene.

Initially, we confirmed *TERT* expression in human embryonic stem cells (ESCs), embryonal carcinoma cells (ECCs), and iPSCs and their parental somatic cells. The *TERT* gene was expressed in pluripotent stem cells including ESCs, ECCs, and iPSCs, but was not detected in any of the parental somatic cells (Fig. 1a).

Analysis of DNA-methylation rates around the *TERT* promoter using DNA-methylation array data appeared to indicate that the distal region (probe positions a-c in Fig. 1b) was more higher methylated in iPSCs than in somatic cells, although little difference was found at the proximal region (probe positions d-f in Fig. 1b) between iPSCs and somatic cells (Fig. 1b). Bisulfite sequencing analysis was performed to further investigate the DNA-methylation state of individual CpG sites around the *TERT* promoter from nt positions -2,056 to +46, which contains 123 CpG sites. Regardless of *TERT* expression and the cell types, the CpG sites located between -610 and +46 nt were rarely methylated and those located between -2,056 and -1,566 nt were highly methylated. However, the CpG sites from -1,415 to -638 nt showed cell type-specific differential methylation. The methylation rates at this region in somatic cells were 20.29%, 29.71%, 34.12%, 40.59%, and 36.18% in AM936EP, Edom22, MRC-5, PAE551, and UtE1104 cells, respectively. In contrast, the methylation rates in pluripotent stem cells were 88.24%, 92.94%, 89.71%, 80.88%, and 72.06% in MRC-iPS-25, PAE-iPS-1, UtE-iPS-6, HUES-8 and NCR-G3 cells, respectively (Fig. 2a). This region includes 34 CpG sites that was highly methylated in ESCs, iPSCs, and ECCs expressing the *TERT* gene, but was hypomethylated in somatic cells lacking *TERT* expression. We designated this region as *TERT*-DMR (*TERT* differentially methylated region).

To gain insight into the correlation between gene expression and DNA methylation, a scatter plot of gene expression versus DNA methylation with pluripotent marker genes

including *POU5F1* (also known as *OCT-4*), *SALL4*, *DPPA4*, and *TERT* of 2 ESCs, 6 iPSCs, and the parental somatic cells were plotted using array data for gene expression and DNA methylation. As expected, *POU5F1*, *SALL4*, and *DPPA4* showed negative correlations (Fig. 2b; $R^2 = 0.8428$, 0.9745, 0.8039, respectively) between DNA methylation and gene expression by linear-regression analysis. These results indicated that *POU5F1*, *SALL4*, and *DPPA4* with hypomethylated promoters were highly expressed in ESCs and iPSCs, whereas low expression of those genes with hypermethylated promoters occurred in the parental somatic cells. Interestingly, *TERT* showed positive correlation (Fig. 2b; $R^2 = 0.9117$) between gene expression and DNA methylation at the distal promoter region, suggesting that in ESCs and iPSCs, *TERT* was highly expressed from hypermethylated promoters and that in the parent somatic cells, *TERT* were poorly expressed from hypomethylated promoters. These results suggested the *TERT* expression is restricted in pluripotent stem cells and that *TERT* expression might be regulated by DNA methylation in manner different than other pluripotent marker genes.

Demethylation led to suppression of the human *TERT* gene

To investigate whether *TERT* expression was regulated by the DNA-methylation status of the *TERT*-DMR, we conducted demethylation assay using MRC-iPSCs. In the demethylation assay, MRC-iPSCs were treated with a demethylating reagent (5-aza-dC) for 4 days, and *TERT* expression was measured. Treatment with 5-aza-dC caused significant demethylation at the *TERT*-DMR (Supplemental Fig. 1) and significant suppression of the *TERT* gene in iPSCs (Fig. 3). Expression of typical stem cell marker genes, POU5F1, NANOG, SOX2, SALL4, and EPHA1 was still maintained in 5-aza-dC-treated iPSCs (Fig. 3). These results suggested that hypermethylation of the *TERT*-DMR is important for maintaining *TERT* expression in iPSCs.

Methylation at the *TERT*-DMR enhanced promoter activity

To further analyze of the effect of DNA methylation at the *TERT*-DMR on *TERT* transcription, region-specific methylated-promoter assays were performed using MRC-iPSCs and the parental somatic cells. We designed four reporter constructs: empty vector (pGL4.10), *TERT*-626, *TERT*-1560, and *TERT*-1560_Me. The DNA sequences of *TERT*-1560 and *TERT*-1560_Me were identical, with the only difference being in their DNA-methylation states. The *TERT*-626 construct, containing the *TERT*-proximal region but not the *TERT*-DMR, showed a significant increase in luciferase activity relative to that of the empty pGL4.10 vector in iPSCs. The *TERT*-1560 construct showed significantly less reporter activity relative to *TERT*-626, being comparable to pGL4.10. Interestingly, the *TERT*-1560_Me construct showed significantly higher reporter activity than the unmethylated construct, *TERT*-1560 (Fig. 4). In the parental somatic cells (MRC-5), none of the constructs showed significantly increased activity relative to that of the pGL4.10. These results suggested that DNA hypermethylation of the *TERT*-DMR was indispensable for *TERT* expression and that he *TERT*-DMR included an expression regulatory element.

Combining the results of the demethylation and methylation assays revealed the possibility that the *TERT*-DMR contained a region that suppress *TERT* expression. Thus, we performed electrophoretic mobility shift assays (EMSA) to determine whether hypermethylation of the *TERT*-DMR prevents certain transcriptional suppressors from binding the *TERT*-DMR. However, no factors that depend on the methylation status were detected (Supplemental Fig. 2a, b).

Methylated *TERT*-DMR maintained open chromatin

Histone modification is another epigenetic mechanism for regulating gene expression. H3K4me3 tends to distribute in "active" gene loci [19], and distribute in hypomethylated DNA region [20]. In contrast, H3K27me3 tends to distribute in "inactive" gene loci [19]. In addition, inactive gene loci are generally enriched for the heterochromatic protein HP-1α and form heterochromatin. The genomic DNA in heterochromatin is usually hypermethylated [21]. Therefore, we performed ChIP-qPCR for H3K4me3, H3K27me3, and HP-1α to determine the histone-modification status at the *TERT*-DMR. ChIP-qPCR revealed that H3K4me3 was significantly enriched in iPSCs, whereas the H3K27me3 and HP-1α were significantly enriched in somatic cells (Fig. 5a-d). Furthermore, analyzing the dataset of ATAC-seq analysis [22] of human ESCs (GSM2433022) [23] and human somatic cells (GSM1939273) revealed that the chromatin structure around the *TERT*-DMR was "open" in *TERT*-expressing pluripotent cells, but was closed in somatic cells. These data indicated that histones at the *TERT*-DMR were active state, even though the DNA was highly methylated in human iPSCs.

Role of hypermethylation of the *TERT*-DMR in regulating *TERT* expression

In human iPSCs that express the *TERT* gene, the *TERT*-DMR was hypermethylated under the active state of histone modification. These results suggested that hypermethylation of the *TERT*-DMR promoted *TERT* expression. To clarify the role of hypermethylation at the *TERT*-DMR in regulating *TERT* gene expression, we searched for factors that interact with the *TERT*-DMR. First, we performed chromosome conformation capture (3C) and Splinkerrete-3C (S3C) assays (see Supplementary methods) to determine whether hypermethylation of the *TERT*-DMR affects the genomic interaction between the *TERT*-DMR and other genomic loci. No genomic interaction was detected (data not shown).

Next, we focused on the nuclear lamina. The nuclear lamina is a polymeric protein meshwork associated with the nucleoplasmic surface of the inner nuclear membrane [24,25] that has been associated with gene silencing by interacting with genomic DNA [26,27]. We performed ChIP-qPCR for Lamin B1, which is a representative component of the nuclear lamina, to determine whether hypermethylation of the *TERT*-DMR inhibited binding to the nuclear lamina. Unexpectedly, Lamin B1 was enriched at the *TERT*-DMR in iPSCs, but not in somatic cells (Fig. 5e), meaning that Lamin B1 was selectively interacted with methylated *TERT*-DMR.

Our findings suggested the model whereby human *TERT* expression is regulated: in the *TERT*-expressing cells such as iPSCs and ESCs, the *TERT*-DMR is highly methylated and binds to the nuclear lamina via Lamin B1, which lead to an open chromatin structure, enabling transcription factors, such as c-MYC [28,29], to bind the proximal promoter and drive *TERT* expression. In contrast, in cells not expressing *TERT* such as most somatic cells, the unmethylated *TERT*-DMR is free in the nucleus. H3K27me3 and HP-1α become enriched at the unmethylated *TERT*-DMR, forming heterochromatin (Fig. 6).

Several groups have discussed the epigenetic regulation of the human *TERT* gene [30–33], however, no clear relationship between DNA methylation and *TERT* expression has been demonstrated. One reason why the epigenetic regulation of *TERT* has been poorly understood may be that previous studies were focused on the proximal core promoter region (approximately 500-bp upstream from the TSS). In this study, we focused on the distal promoter region of the *TERT* gene and identified the *TERT*-DMR, provides additional information for the human *TERT* gene.

Of note, the demethylating regent 5-aza-dC (also known as decitabine) has been used clinically for treating acute myeloid leukemia (AML) in patients whose malignant cells express [34]. In addition, treatment with decitabine has been reported to suppresses

expression and inhibits malignant cell proliferation [35,36]. However, exactly how decitabine suppresses *TERT* expression remains unclear. In this study, demethylating *TERT*-DMR with 5-aza-dC suppressed of *TERT* expression. Therefore, the therapeutic effect of decitabine in AML potentially involves the inhibition of *TERT* expression through *TERT*-DMR demethylation. Moreover, monitoring DNA methylation at the *TERT*-DMR may be useful for diagnosis, prognosis, and as a biomarker for estimating the risk for developing AML.

In conclusion, we identified *TERT*-DMR at the distal *TERT* promoter region. Hypermethylation of the *TERT*-DMR promoted activation of *TERT* gene expression by binding to the nuclear membrane. Our findings shed light on a new functional aspect of DNA methylation with respect to gene expression. This novel epigenetic regulation mechanism is required for the reprogramming the transformation of somatic cells into iPSCs.

Acknowledgments

We would like to express our sincere thanks to Drs. C. Cowan and T. Tenzan for the HUESC lines; to Drs. N. Hattori and J. Tomikawa for assistance with the ChIP and 3C method, respectively; to Dr. S. Wakitani for discussion. This study was funded by a Grant-in-Aid for the Japan Society for the Promotion of Science (JSPS) Research Fellow (No. JP15J11596 to K.T), a Grant-in-Aid for Scientific Research (B) (No. 25292187 to K.N.), and a Grant-in-Aid for challenging Exploratory Research (No. 16K15055 to K.N.) from the JSPS KAKENHI; and by funding to K.N. from The NOVARTIS Foundation (Japan) for the Promotion of Science, the Terumo Foundation grant, and the Takeda Science Foundation.

Compliance with ethical standards

Conflict of interest

The authors declare that they have no conflict of interest.

Ethical approval

This study was approved by the research ethics committee of Miyazaki University and Institutional Review Board of the National Institute for Child Health and Development. All procedures performed in studied involving the handling of human cells were in accordance with the ethical standards of the 1964 Helsinki declaration and its later amendments or comparable ethical standard.

References

1. K. Takahashi, K. Tanabe, M. Ohnuki, M. Narita, T. Ichisaka, K. Tomoda, et al., Induction of pluripotent stem cells from adult human fibroblasts by defined factors., Cell. 2007;131:861–72.
2. T. Imamura, J. Ohgane, S. Ito, T. Ogawa, N. Hattori, S. Tanaka, et al., CpG island of rat sphingosine kinase-1 gene: tissue-dependent DNA methylation status and multiple alternative first exons., Genomics. 2001;76:117–125.
3. C.K. Shen, T. Maniatis, Tissue-specific DNA methylation in a cluster of rabbit beta-like globin genes., Proc. Natl. Acad. Sci. 1980;77(11):6634–6638.
4. Y.-G.G. Ko, K. Nishino, N. Hattori, Y. Arai, S. Tanaka, K. Shiota, Stage-by-stage change in DNA methylation status of Dnmt1 locus during mouse early development., J. Biol. Chem. 2005;280:9627–9634.
5. K. Nishino, N. Hattori, S. Tanaka, K. Shiota, DNA methylation-mediated control of Sry gene expression in mouse gonadal development., J. Biol. Chem. 2004;279:22306–22313.
6. K. Nishino, M. Toyoda, M. Yamazaki-Inoue, H. Makino, Y. Fukawatase, E. Chikazawa, et al., Defining hypo-methylated regions of stem cell-specific promoters in human iPS cells derived from extra-embryonic amnions and lung fibroblasts., PLoS One. 2010;5:e13017.
7. K. Takahashi, S. Yamanaka, Induction of Pluripotent Stem Cells from Mouse Embryonic and Adult Fibroblast Cultures by Defined Factors, Cell. 2006;126:663–676.
8. C.-H. Cui, T. Uyama, K. Miyado, M. Terai, S. Kyo, T. Kiyono, et al., Menstrual blood-derived cells confer human dystrophin expression in the murine model of Duchenne muscular dystrophy via cell fusion and myogenic transdifferentiation., Mol. Biol. Cell. 2007;18:1586–1594.

9. S. Nagata, M. Toyoda, S. Yamaguchi, K. Hirano, H. Makino, K. Nishino, et al., Efficient reprogramming of human and mouse primary extra-embryonic cells to pluripotent stem cells., Genes to Cells. 2009;14:1395–1404.

10. J.P. Jacobs, C.M. Jones, J.P. Baille, Characteristics of a human diploid cell designated MRC-5., Nature. 1970;227:168–170.

11. J. Hata, J. Fujimoto, E. Ishii, A. Umezawa, Y. Kokai, Y. Matsubayashi, et al., Differentiation of human germ cell tumor cells in vivo and in vitro, Acta Histochem. Cytochem. 1992;25:563–576.

12. H. Makino, M. Toyoda, K. Matsumoto, H. Saito, K. Nishino, Y. Fukawatase, et al., Mesenchymal to embryonic incomplete transition of human cells by chimeric OCT4/3 (POU5F1) with physiological co-activator EWS, Exp. Cell Res. 2009;315:2727–2740.

13. K. Nishino, M. Toyoda, M. Yamazaki-Inoue, Y. Fukawatase, E. Chikazawa, H. Sakaguchi, et al., DNA methylation dynamics in human induced pluripotent stem cells over time., PLoS Genet. 2011;7:e1002085.

14. C.A. Cowan, I. Klimanskaya, J. McMahon, J. Atienza, J. Witmyer, J.P. Zucker, et al., Derivation of embryonic stem-cell lines from human blastocysts., N. Engl. J. Med. 2004;350:1353–1356.

15. K.J. Livak, T.D. Schmittgen, Analysis of relative gene expression data using real-time quantitative PCR and the 2(-Delta Delta C(T)) Method., Methods. 2001;25:402–408.

16. H. Tateno, A. Matsushima, K. Hiemori, Y. Onuma, Y. Ito, K. Hasehira, et al., Podocalyxin Is a Glycoprotein Ligand of the Human Pluripotent Stem Cell-Specific Probe rBC2LCN, Stem Cells Transl. Med. 2013;2:265–273.

17. Y. Kumaki, M. Oda, M. Okano, QUMA: quantification tool for methylation analysis., Nucleic Acids Res. 2008;36:W170-5. doi: 10.1093/nar/gkn294

18. X. Lin, L. Tirichine, C. Bowler, F. Round, R. Crawford, D. Mann, et al., Protocol: Chromatin immunoprecipitation (ChIP) methodology to investigate histone modifications in two model diatom species, Plant Methods. 2012;8:48.

19. A.P. Bracken, N. Dietrich, D. Pasini, K.H. Hansen, K. Helin, Genome-wide mapping of Polycomb target genes unravels their roles in cell fate transitions., Genes Dev. 2006;20:1123–1136.

20. D.-S. Lee, J.-Y. Shin, P.D. Tonge, M.C. Puri, S. Lee, H. Park, et al., An epigenomic roadmap to induced pluripotency reveals DNA methylation as a reprogramming modulator, Nat. Commun. 2014;5:5619.

21. N.R. Rose, R.J. Klose, Understanding the relationship between DNA methylation and histone lysine methylation, BBA - Gene Regul. Mech. 2014;1839:1362–1372.

22. J.D. Buenrostro, B. Wu, H.Y. Chang, W.J. Greenleaf, ATAC-seq: A Method for Assaying Chromatin Accessibility Genome-Wide., Curr. Protoc. Mol. Biol. 2015;109:21.29.1-9.

23. G. Boulay, M.E. Awad, N. Riggi, T.C. Archer, S. Iyer, W.E. Boonseng, et al., OTX2 Activity at Distal Regulatory Elements Shapes the Chromatin Landscape of Group 3 Medulloblastoma., Cancer Discov. 2017; 7:288–301.

24. V. Butin-Israeli, S.A. Adam, A.E. Goldman, R.D. Goldman, Nuclear lamin functions and disease., Trends Genet. 2012; 28:464–471.

25. T. Dechat, S.A. Adam, P. Taimen, T. Shimi, R.D. Goldman, Nuclear lamins., Cold Spring Harb. Perspect. Biol. 2010;2:a000547–a000547.

26. B. Burke, C.L. Stewart, The nuclear lamins: flexibility in function., Nat. Rev. Mol. Cell Biol. 2013;14:13–24.

27. Y.Y. Shevelyov, D.I. Nurminsky, The nuclear lamina as a gene-silencing hub., Curr. Issues Mol. Biol. 2012;14:27–38.

28. I. Horikawa, P.L. Cable, C. Afshari, J.C. Barrett, Cloning and characterization of the promoter region of human telomerase reverse transcriptase gene., Cancer Res. 1999;59:826–830.

29. K.J. Wu, C. Grandori, M. Amacker, N. Simon-Vermot, a Polack, J. Lingner, et al., Direct activation of TERT transcription by c-MYC., Nat. Genet. 1999;21:220–4.

30. I. Guilleret, J. Benhattar, Unusual distribution of DNA methylation within the hTERT CpG island in tissues and cell lines., Biochem. Biophys. Res. Commun. 2004;325:1037–43.

31. N.G. Lopatina, J.C. Poole, S.N. Saldanha, N.J. Hansen, J.S. Key, M. a Pita, et al., Control mechanisms in the regulation of telomerase reverse transcriptase expression in differentiating human teratocarcinoma cells, Biochem. Biophys. Res. Commun. 2003;306:650–659.

32. I. Guilleret, P. Yan, F. Grange, R. Braunschweig, F.T. Bosman, J. Benhattar, Hypermethylation of the human telomerase catalytic subunit (hTERT) gene correlates with telomerase activity., Int. J. Cancer. 2002;101:335–41.

33. S.K. Dessain, H. Yu, R.R. Reddel, R.L. Beijersbergen, R.A. Weinberg, Methylation of the human telomerase gene CpG island., Cancer Res. 2000;60:537–41.

34. M. Nieto, P. Demolis, E. Béhanzin, A. Moreau, I. Hudson, B. Flores, et al., The European Medicines Agency Review of Decitabine (Dacogen) for the treatment of adult patients with acute myeloid leukemia: summary of the scientific assessment of the committee for medicinal products for human use., Oncologist. 2016;21:692–700.

35. M. Hájek, I. Votruba, A. Holý, M. Krecmerová, E. Tloust'ová, Alpha anomer of 5-aza-2'-deoxycytidine down-regulates hTERT mRNA expression in human leukemia HL-60 cells., Biochem. Pharmacol. 2008;75:965–72.

36. K.A. Pettigrew, R.N. Armstrong, H.A.A. Colyer, S. Zhang, I.M. Rea, R.E. Jones, et al., Differential TERT Promoter Methylation and Response to 5-Aza-2 0 -deoxycytidine in Acute Myeloid Leukemia Cell Lines : TERT Expression , Telomerase Activity , Telomere Length , and Cell Death, Genes. Chromosomes Cancer. 2012;780:768–780.

Figure legends

Fig. 1. Expression of the human *TERT* gene and DNA methylation of the *TERT* promoter region.

(a) Expression of the *TERT* gene in 5 somatic, 6 iPSC, 4 ESC, and 2 ECC lines, as detected by RT-PCR. The upper and lower panels show *TERT* and GAPDH expression, respectively. (b) DNA-methylation rate at the *TERT* promoter region in parental somatic cells and pluripotent stem cells. (Top) Diagram of the *TERT* gene. The white box indicates the 1st exon of the *TERT* gene. The position of the transcription start site (TSS) was designated as +1. Black vertical lines (a-f) indicate the position of each probe. The probe identification numbers of a-f are cg07380026 (-845), cg26006951 (-826), cg17166338 (-807), cg10767223 (-637), cg11625005 (-575), and cg10896616 (-105), respectively. (Bottom) DNA-methylation levels were determined with the Illumina Infinium HumanMethylation450K assay. The relative ratios of methylated and unmethylated DNA are indicated by the black and white areas, respectively, in the pie chart. PSCs, pluripotent stem cells.

Fig. 2. Bisulfite sequencing analysis and correlation between DNA methylation and gene expression.

(a) Bisulfite sequencing analysis of the 5'-flanking regions of the *TERT* gene. (Top) Diagram of the *TERT* gene. The white box indicates the 1st exon of the *TERT* gene. Black vertical lines indicate the position of individual CpG sites. The position of the TSS was designated as +1. Black horizontal lines (T1-T6) indicate the regions studied by bisulfite sequencing. (Bottom) The open and closed circles indicate the unmethylated and methylated states of each CpG site, respectively. Black arrowheads represent the position of each CpG site in Infinium HumanMethylation450K assay (cg07380026). The horizontal line at the bottom of the figure indicates the defined *TERT*-DMR extending from nt positions -1,415 to -

638 nt. (b) Scatter plot of DNA methylation and gene-expression levels for *POU5F1*, *SALL4*, *DPPA4*, and *TERT*. DNA-methylation levels were determined by performing the Illumina Infinium HumanMethylation450K assay. The methylation probes used for *POU5F1*, *SALL4*, *DPPA4*, and *TERT* (shown in the plot) are cg15948871, cg10941835, cg14836960, and cg07380026, respectively. White triangles, iPSCs (n = 6). White inverted triangles, ESCs (n = 2). Black circles, somatic cells (n = 5). Black lines, linear-regression lines.

Fig. 3. Demethylation of the *TERT*-DMR led to suppressed of *TERT* expression.

Effect of a demethylation reagent (5-aza-dC) on the expression of *TERT* and pluripotent marker genes in MRC-iPSCs. (Top) *TERT*, *POU5F1*, *NANOG*, *SOX2*, *SALL4*, *EPHA1*, and *GAPDH* gene expression. *GAPDH* was detected as an internal control. (Bottom) Relative TERT gene-expression levels measured by qPCR, with normalization to *GAPDH* expression using the delta-delta CT method. The data shown represent the means ± S.E. *$p < 0.01$.

Fig. 4. Methylation of the *TERT*-DMR enhanced the promoter activity.

Region-specific methylated-reporter assay in MRC-iPSCs and parental somatic cells (MRC-5). (Top) Schematic representation of the TERT gene and reporter constructs. Open and closed circles indicate unmethylated and methylated CpG sites in the constructs, respectively. (Bottom) Luciferase activity of each reporter construct. White bars indicate luciferase activities in parent somatic cells (MRC-5). Black bars indicate luciferase activities in MRC-iPSCs. Each bar shown in the figure represents the mean ± SEM. *$p < 0.05$

Fig. 5. ChIP-qPCR at the *TERT*-DMR and neighboring region.

(a) Schematic diagram of the 5′-flanking region of *TERT*. Horizontal black bars indicate regions targeted by ChIP-qPCR. The white box indicates the 1st exon of the *TERT* gene. (b–e)

ChIP-qPCR for H3K4me3 (b), H3K27me3 (c), HP-1α (d), and Lamin B1 (e) in somatic cells (MRC-5) and MRC-iPSCs. Enrichment at each position is indicated as normalized percent-input (IgG-subtracted). The white and black bars indicate data from parent somatic cells and iPSCs, respectively. Each bar shown in the figure represents the mean ± SEM. *$p < 0.05$.

Fig. 6. Model of *TERT* expression regulated by *TERT*-DMR hypermethylation.

Schematic representation shown our proposed model whereby *TERT* expression is regulated by hypermethylation of the *TERT*-DMR. (Top) In *TERT*-expressing cells, such as iPSCs and ESCs, the *TERT*-DMR is highly methylated and binds to Lamin B1, a component of the nuclear lamina, which leads to an open chromatin structure and enables c-MYC to bind the proximal promoter for *TERT* expression. (Bottom) In cells not expressing *TERT*, such as most somatic cells, the unmethylated *TERT*-DMR is free in the nucleus. H3K27me3 and HP-1α become enriched at the unmethylated *TERT*-DMR, forming heterochromatin.

Figure_1

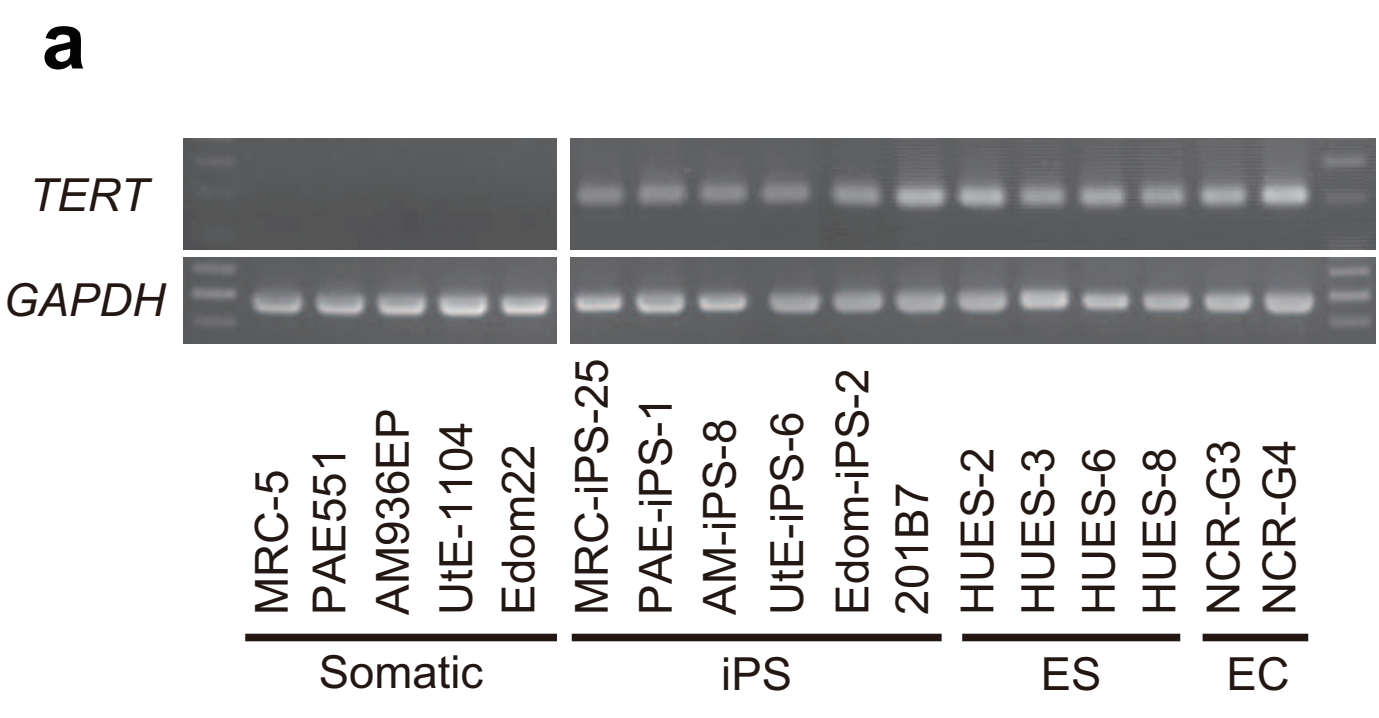
a
TERT
GAPDH
MRC-5
PAE551
AM936EP
UtE-1104
Edom22
MRC-iPS-25
PAE-iPS-1
AM-iPS-8
UtE-iPS-6
Edom-iPS-2
201B7
HUES-2
HUES-3
HUES-6
HUES-8
NCR-G3
NCR-G4
Somatic
iPS
ES
EC

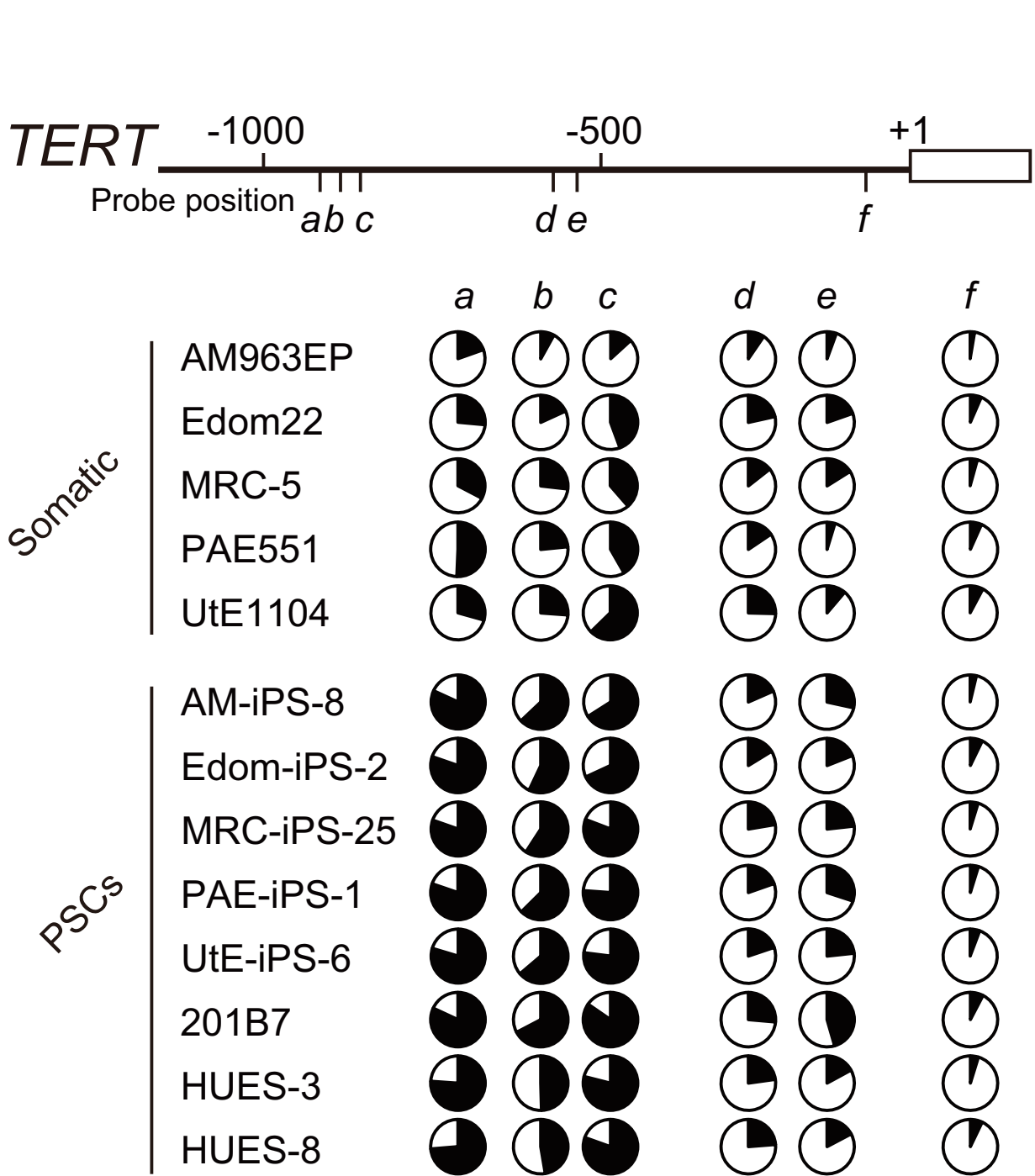
b
TERT
-1000
-500
+1
Probe position
a b c
d e
f
a b c d e f
Somatic
AM963EP
Edom22
MRC-5
PAE551
UtE1104
PSCs
AM-iPS-8
Edom-iPS-2
MRC-iPS-25
PAE-iPS-1
UtE-iPS-6
201B7
HUES-3
HUES-8

Figure_2

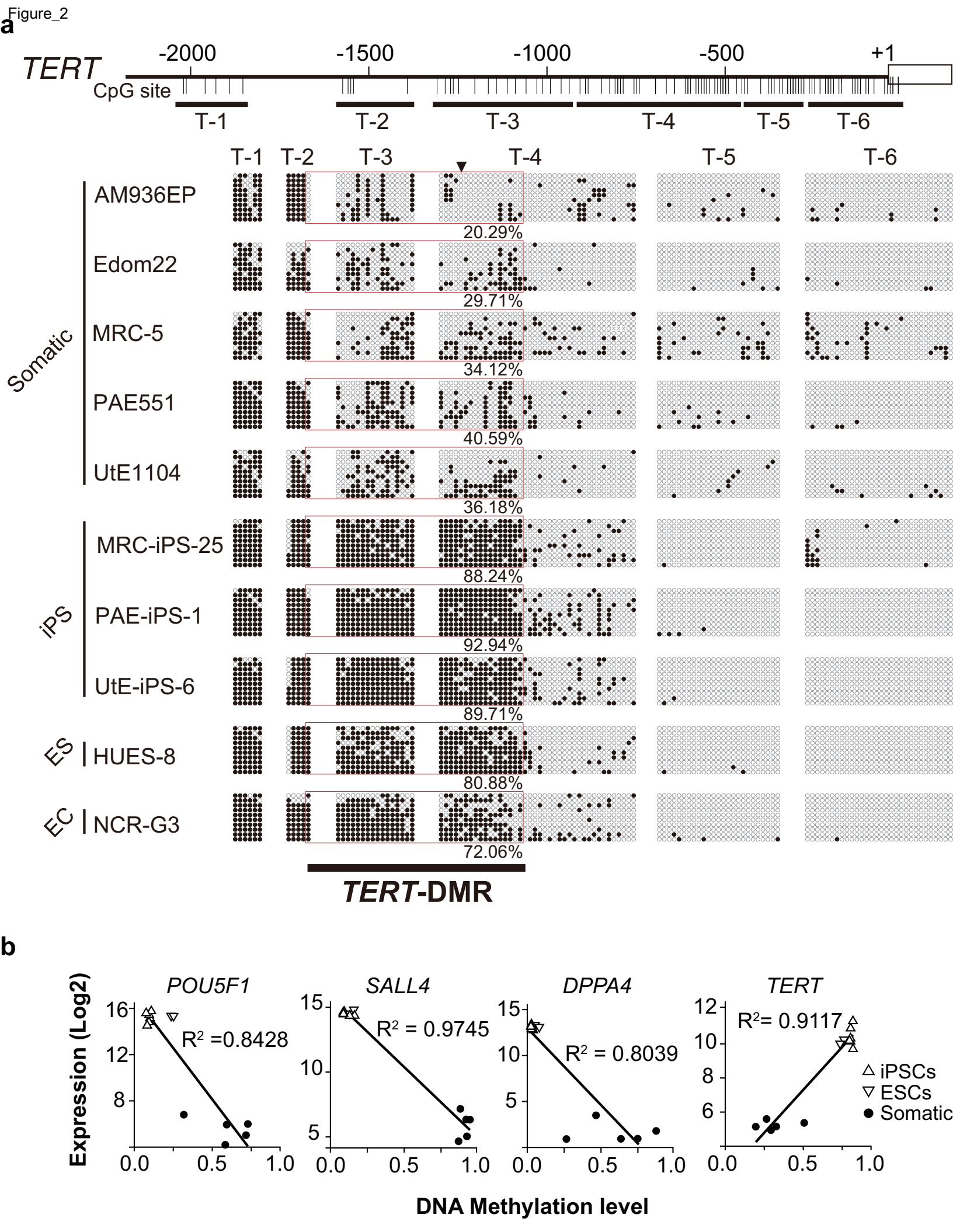
a
TERT
-2000
-1500
-1000
-500
+1
CpG site
T-1
T-2
T-3
T-4
T-5
T-6
Somatic
AM936EP
20.29%
Edom22
29.71%
MRC-5
34.12%
PAE551
40.59%
UtE1104
36.18%
iPS
MRC-iPS-25
88.24%
PAE-iPS-1
92.94%
UtE-iPS-6
89.71%
ES
HUES-8
80.88%
EC
NCR-G3
72.06%
TERT-DMR
b
POU5F1
SALL4
DPPA4
TERT
R² =0.8428
R² = 0.9745
R² = 0.8039
R²= 0.9117
Expression (Log2)
DNA Methylation level
iPSCs
ESCs
Somatic

Figure_3

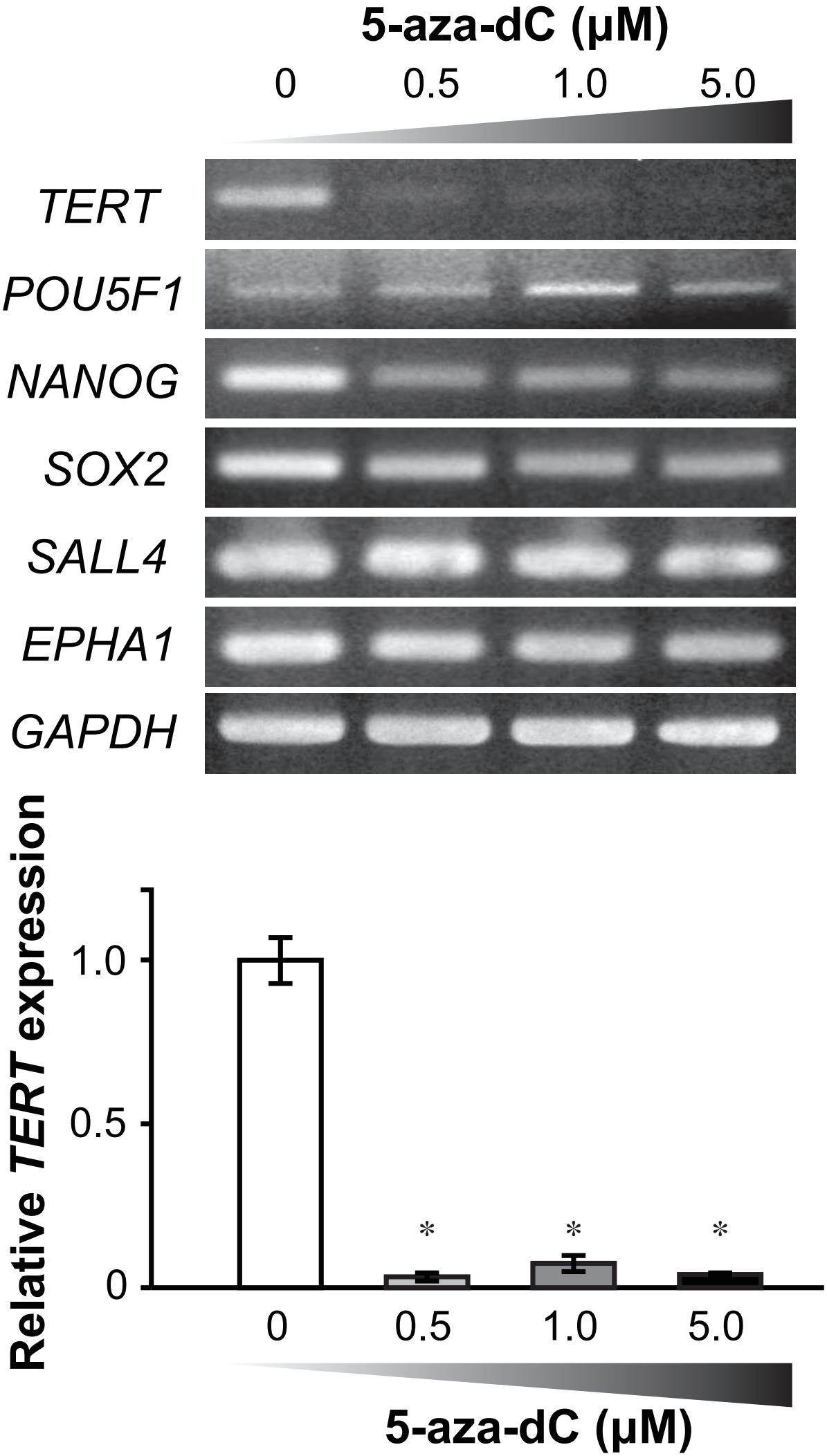
5-aza-dC (μM)
0
0.5
1.0
5.0
TERT
POU5F1
NANOG
SOX2
SALL4
EPHA1
GAPDH
Relative TERT expression
1.0
0.5
0
*
*
*
0
0.5
1.0
5.0
5-aza-dC (μM)

Figure_4

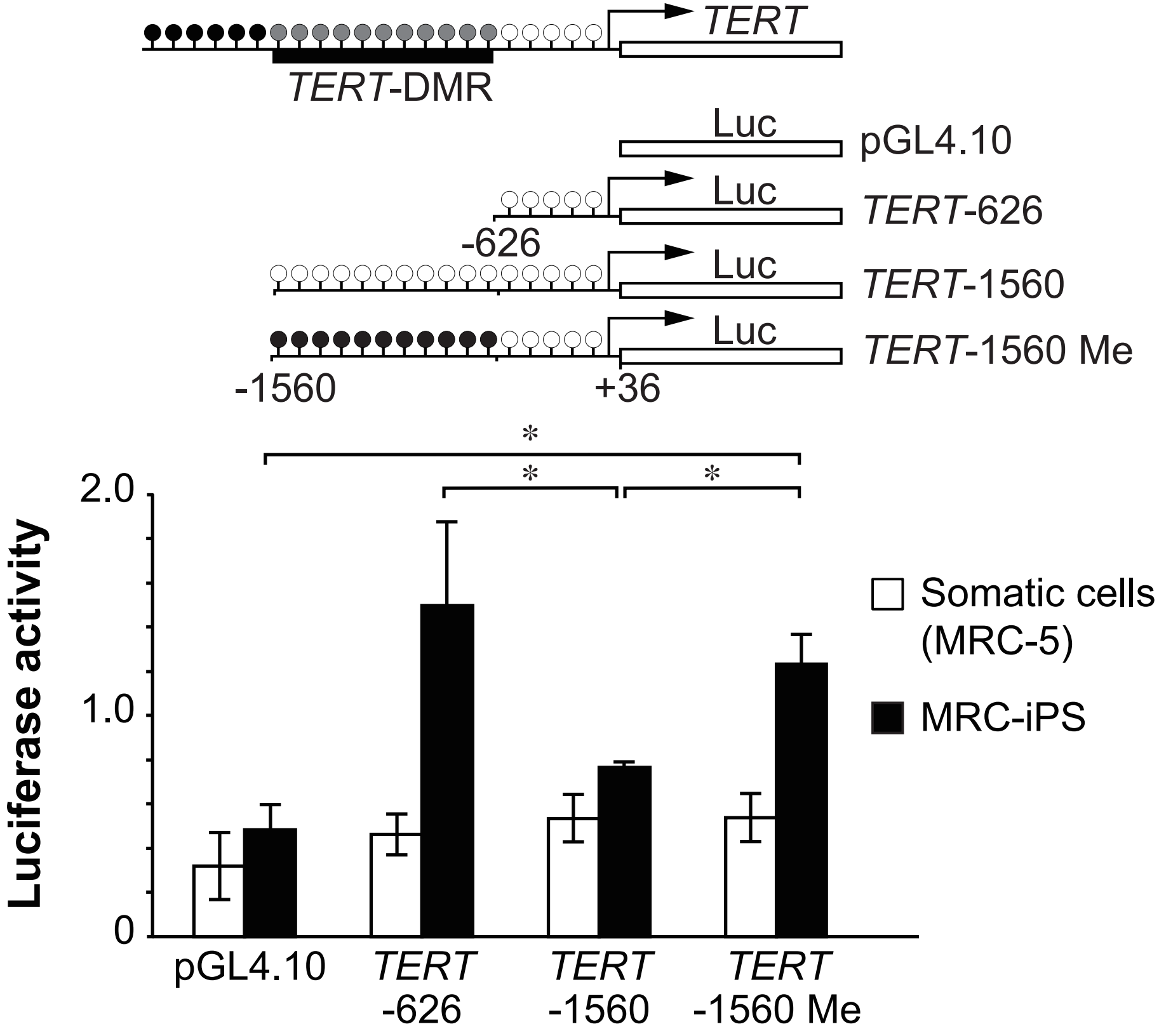
TERT
TERT-DMR
Luc
pGL4.10
Luc
TERT-626
-626
Luc
TERT-1560
Luc
TERT-1560 Me
-1560
+36
*
*
*
2.0
1.0
0
Luciferase activity
Somatic cells (MRC-5)
MRC-iPS
pGL4.10
TERT -626
TERT -1560
TERT -1560 Me

Figure_5

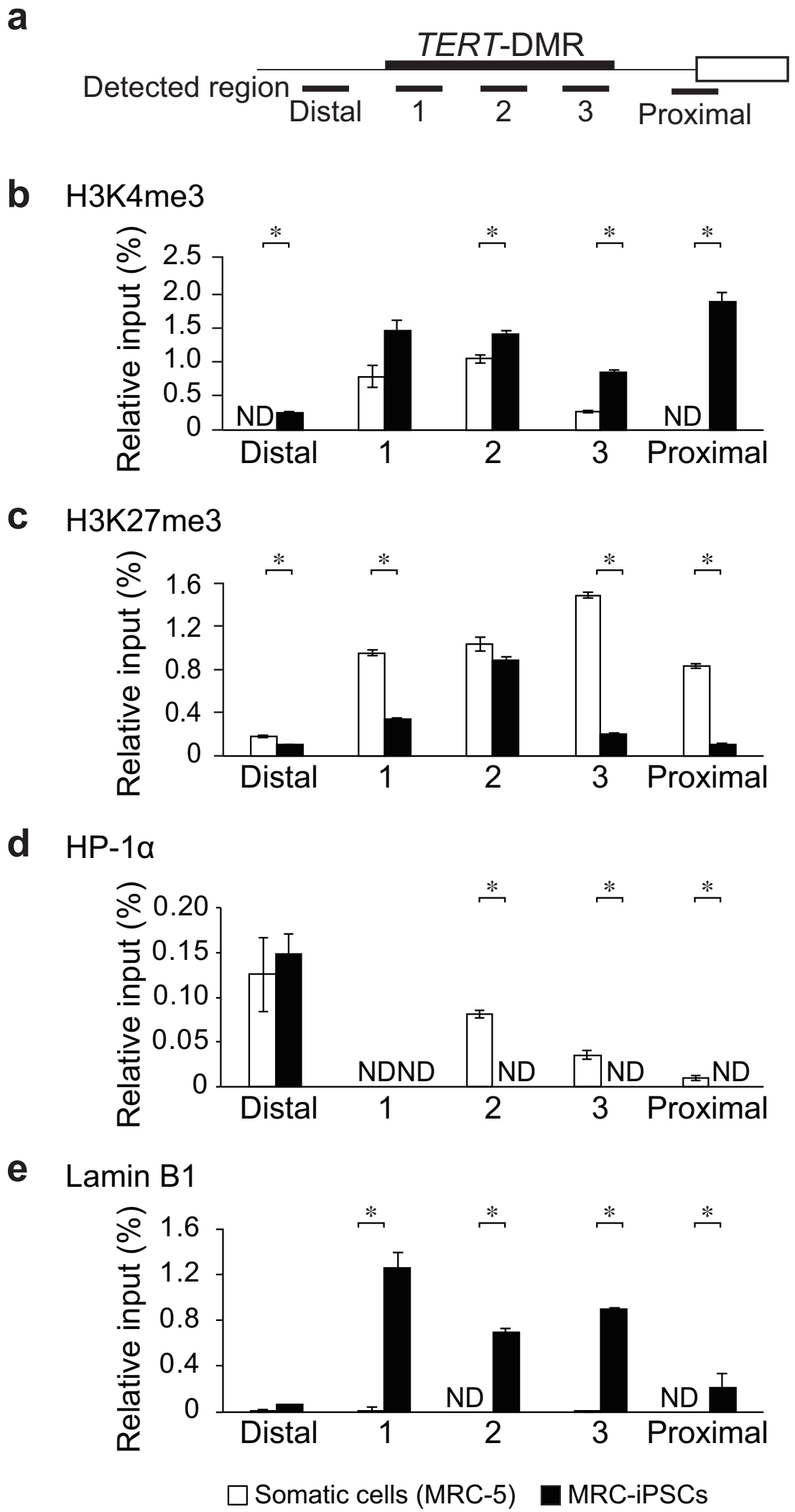
a
TERT-DMR
Detected region
Distal
1
2
3
Proximal
b
H3K4me3
Relative input (%)
2.5
2.0
1.5
1.0
0.5
0
ND
ND
Distal
1
2
3
Proximal
c
H3K27me3
Relative input (%)
1.6
1.2
0.8
0.4
0
Distal
1
2
3
Proximal
d
HP-1α
Relative input (%)
0.20
0.15
0.10
0.05
0
NDND
ND
ND
ND
Distal
1
2
3
Proximal
e
Lamin B1
Relative input (%)
1.6
1.2
0.8
0.4
0
ND
ND
Distal
1
2
3
Proximal
Somatic cells (MRC-5)
MRC-iPSCs

Figure_6

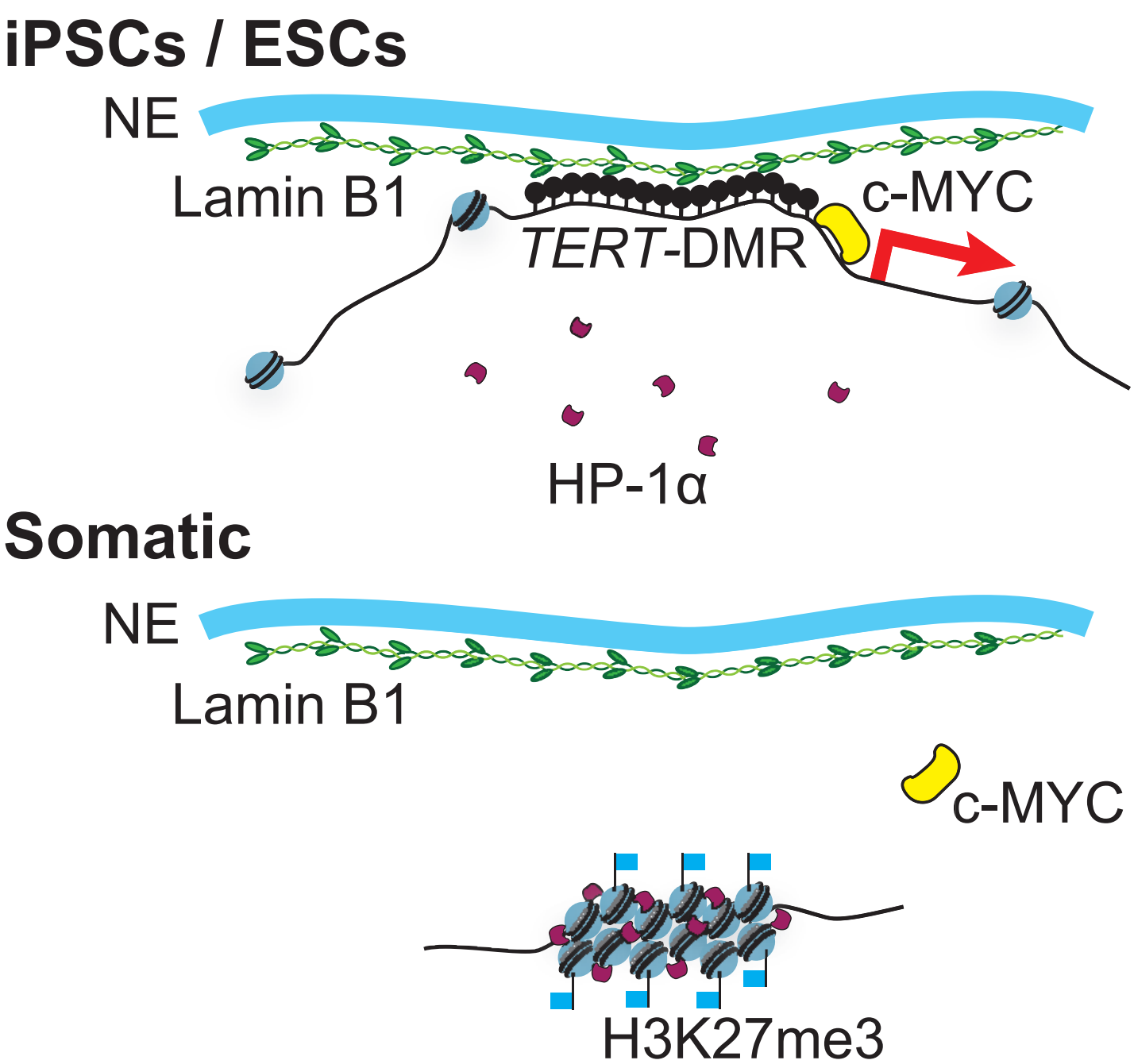
iPSCs / ESCs
NE
Lamin B1
c-MYC
TERT-DMR
HP-1α
Somatic
NE
Lamin B1
c-MYC
H3K27me3